Relationship between the equatorial and meridional modes of climatic variability in the tropical Atlantic

Jacques Servain[1], Ilana Wainer[2], Julian P. McCreary[3] Jr., Alain Dessier[1]

Abstract. The tropical Atlantic Ocean exhibits two primary modes of interannual climate variability: an equatorial mode analogous to, but weaker than, the Pacific El Niño phenomenon, and a meridional mode that does not have a Pacific counterpart. The equatorial mode is responsible for warm (and cold) sea surface temperature (SST) events, mainly in the Gulf of Guinea, and is identifiable by abnormal changes in the equatorial thermocline slope resulting from zonal-wind anomalies in the western tropical Atlantic. The meridional mode is characterized by a north-south interhemispheric gradient of SST anomalies. Here it is shown, using observed surface and subsurface oceanic temperatures, that the meridional mode is linked to the equatorial mode, at both decadal and short-interannual (1-2 years) time scales. Both modes involve north-south displacements of the ITCZ, as in the annual response.

Introduction

During the last decade, a number of studies have identified two primary modes of climate variability in the tropical Atlantic (see, for example, Servain and Merle, 1993). One of them, the equatorial mode, is known to have time scales that vary from a few months to 2–4 years. It is similar to, albeit much weaker than, the Pacific El Niño-Southern Oscillation (ENSO) in that it relates changes in the tropical ocean's thermal structure to trade-wind anomalies in the western equatorial ocean. Specifically, when the trades intensify (weaken) in the western Atlantic, the equatorial thermocline slope increases (decreases), and negative (positive) SST anomalies develop in the equatorial ocean, particularly in the Gulf of Guinea (Servain and Arnault, 1995). It has a significant societal impact because it affects the distribution and intensity of precipitation in the African monsoon (Hisard, 1980).

The Atlantic meridional mode has no Pacific counterpart. It is characterized by a north-south interhemispheric gradient of SST anomalies. It exhibits interannual to decadal time scales (Moura and Shukla, 1981; Servain, 1991; Mehta and Delworth, 1995; Rajagopalan et al., 1998) and has been referred to as the "dipole mode" During typical dipole episodes (i.e. the simultaneous manifestation of the out-of-phase relationship in the tropical Atlantic SST), anomalies appear with opposite signs on either side of the Intertropical Convergence Zone (ITCZ). However, their development is not always simultaneous (Houghton and Tourre, 1992). So far, this mode has been observed mainly in SST and surface wind fields, and little is known about its subsurface manifestations. It also has a societal impact, most notably through its effect on droughts in Northeast Brazil (Servain, 1991; Wainer and Soares, 1997) and the Sahel region (Folland et al., 1986).

In this paper, we use observed oceanic temperature data to address the question of whether the two modes interact with each other, and if so at what preferential frequencies. Based on the cross-correlations between each mode, we find that they interact at both decadal and short-interannual (1-2 years) time scales. Furthermore, the interaction is associated with anomalous north-south shifts in the location of the ITCZ, similar to what happens in the seasonal cycle.

[1] Centre ORSTOM de Brest, Plouzané, France
[2] Dept. Oceanográfia Fisíca, Universidade de São Paulo, São Paulo, Brazil
[3] Oceanographic Center, Nova Southeastern University, Dania, USA

Paper number 1999GL900014.
0094-8276/99/1999GL900014$05.00

Data sources

Owing to the increasing amount of surface marine observations obtained from the tropical-Atlantic Volunteer Observing Ship (VOS) system, SST and surface wind data are sufficient to determine monthly maps on a 2° x 2° grid since 1964 (Servain et al., 1985, 1996). In contrast, it is not yet possible to obtain a continuous basin-wide picture of the observed oceanic properties below the ocean's surface. Historical subsurface data are obtained mainly from expendable bathythermograph (XBT) drops. As for the surface data set, these observations are available from the VOS system, but in far fewer numbers, and their coverage is restricted primary to ship tracks. In the tropical Atlantic, two ship tracks, AX11 (Europe-South America) and AX15 (Europe-South Africa), shown in Figure 1, are sampled densely enough to allow continuous monthly coverage since the beginning of the 1980's, when intensive subsurface observations first began to be taken (Fabri et al., 1996). For this reason, the analyses in the results section are restricted to the period 1980–1997.

Overview

Equatorial mode

To provide a visualization of the overall spatial structure of the equatorial mode, Figure 1 shows a pattern of thermocline depth anomalies obtained from a solution to an oceanic general circulation model (Delécluse et al., 1993). The figure shows the first empirical orthogonal function (EOF) of the 20°C depth anomaly, which is a typical temperature of the mid-thermocline within the tropics. A similar, but much less complete pattern is derivable from the few available observations (see, for example, Reverdin et al., 1991). Hereafter, the 20°C-isotherm depth and the 20°C-isotherm depth anomaly, are designated by D20 and Z20, respectively. Positive (negative) values of Z20 are related to an abnormal deepening (shallowing) of D20.

It is well known that ocean dynamics play a prominent role in the generation of Z20 patterns like those in Figure 1, as well as in the development of interannual SST anomalies in the eastern equatorial ocean. These dynamical processes are therefore likely to be important in the equatorial mode itself. Consider the response to strengthened trade winds in the western ocean: they induce a more pronounced deepening of D20 in the western

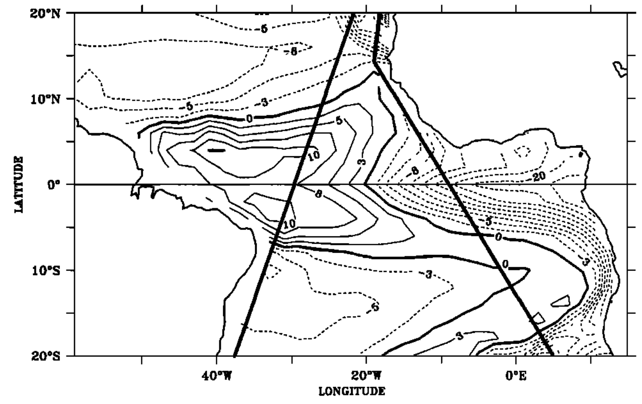

Figure 1. Spatial structure of the first EOF of Z20 monthly anomalies from the numerical solution of Delécluse et al. (1993). Straight lines indicate ship tracks AX11 (west) and AX15 (east).

equatorial ocean (Z20 > 0), excite equatorially trapped Kelvin waves that propagate eastward across the basin in a few weeks time, lifting the thermocline in the eastern equatorial ocean (Z20 < 0), and consequently increasing the equatorial tilt of D20. These waves subsequently reflect from the eastern boundary as Rossby waves and coastal Kelvin waves, thereby extending the response throughout the eastern ocean and to latitudes well off the equator. Because the thermocline shallows throughout the eastern ocean, cool subsurface water is able to upwell to the surface more readily, creating cold SST anomalies in the region. The pattern in Figure 1 results from such processes, and its opposite occurs in response to weakened trades. Observational evidence for this type of dynamical response can be found in Moore et al. (1978), Picaut (1983), and Katz (1987, 1997). More detailed discussions of the relevant theory can be found in Philander (1979), McCreary et al. (1984), Zebiak (1993) and Servain and Arnault (1995).

Dipole mode

Figure 2 illustrates the north-south interhemispheric gradient of SST anomalies (hereafter referred to as the dipole mode) It depicts the first EOF of SST from the same numerical solution as before. The pattern exhibits a dipole structure with opposite SST anomalies on either side of the mean position of the ITCZ. It is consistent with patterns determined from observations (see, for example, Moura and Shukla, 1981, or Nobre and Shukla, 1996), differing primarily in that the two cores of the dipole are located nearer to the equator in the numerical solution.

In contrast to the equatorial mode, the ocean dynamics associated with this dipole mode are not well understood. Indeed, recent studies suggest that it has a purely thermodynamic origin (Carton et al., 1996; Chang et al., 1997). Nevertheless, even if ocean thermodynamics is instrumental in determining the origin of the interhemispheric SST anomalies, dynamical processes are likely to play some role. In the Chang et al. (1997) coupled model, for example, although positive feedback is generated thermodynamically by a mutual interaction between the wind-induced heat flux and SST, ocean dynamics (temperature advection) provides the negative feedback that sets the long time scale of the variability.

Results

As noted above, the equatorial mode is characterized by abnormal changes in the west-east slope of the equatorial thermocline. To estimate this slope anomaly from observations, we utilized the 1980–1997 XBT data along the AX11 and AX15 tracks (Figure 1), filtered to remove the climatological annual cycle. These time series give Z20 at two locations on the equator: close to 30°W for AX11 and close to 10°W for AX15. Subtracting the eastern time series from the western one provides a measure of the equatorial thermocline slope anomaly (ΔZ20), with positive (negative) values of ΔZ20 corresponding to a larger (smaller) equatorial slope.

The dipole mode is commonly characterized by interhemispheric SST anomalies with opposite signs on either side of the ITCZ. To measure this gradient, we subtract the monthly anomalous SST averaged between 5°N–20°S from that averaged between 5°–30°N (ΔSST). With this choice, positive (negative) values of ΔSST correspond to a SST dipole pattern that is positive (negative) in the northern ocean and negative (positive) in the equatorial and southern regions. Thus, the dipole index must be considered here as a simple measure of the meridional gradient in the SST anomaly pattern. ΔSST is based solely on monthly SST observations, equitably integrated throughout the entire tropical basin, and does not involve any statistical processing (e.g., normal or rotated EOFs). In such a calculation, the northern part has exactly the same weight as the southern part (which includes the equatorial domain). It has been shown that this simple arithmetical dipole index has consistency and utility in its relationship with climatic variations in the Sahel and Nordeste regions (Servain, 1991).

We also determine a monthly index of the anomalous latitudinal position of the ITCZ, ΔITCZ, for the same period 1980–1997. It is defined to be the abnormal latitudinal displacement of the zero value of the meridional wind along 28°W, a meridian near the center of the basin. Positive (negative) values of ΔITCZ identify a northward (southward) abnormal position of ITCZ, and are basically related to a strengthening (decrease) of the southeast trades and a decrease (strengthening) of the northeast trades (Servain and Merle, 1993).

The three indices (ΔZ20, ΔSST and ΔITCZ) are plotted in Figure 3, smoothed by a 6-month running-mean filter. Large interannual oscillations, in which the SST dipole evolves from a positive to a negative state and returns, can be seen during the study period. At the same time, the tilt of Z20 along the equator evolves similarly, from positive conditions (a pronounced slope) to negative conditions (a flat thermocline) and returns. ΔSST and ΔZ20 are well correlated, with the maximum correlation coefficient between equal to 0.54 at 1-month lag (ΔZ20 leading).

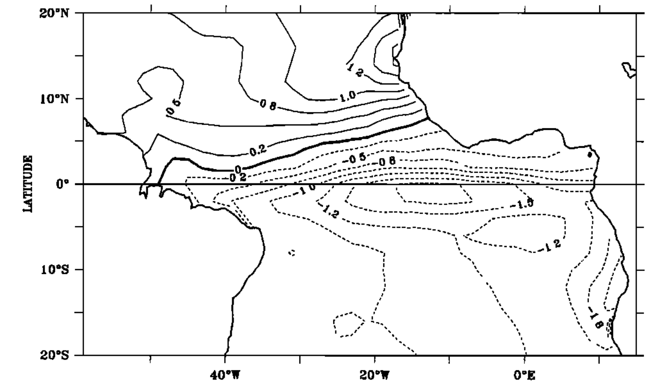

Figure 2. Spatial structure of the first EOF of SST monthly anomalies from the numerical solution of Delécluse et al. (1993).

This indicates that the equatorial and dipole modes are significantly linked at climatic time scales.

The correlation coefficient between ΔITCZ and ΔSST is also high (maximum correlation of 0.73 with a 1-month lag (ITCZ leading): a northward (southward) deviation of ITCZ corresponds to a positive (negative) SST dipole pattern. The correlation between ΔITCZ and ΔZ20 is weaker (a maximum coefficient of 0.45 at 0 lag), although the two time series exhibit similar temporal evolution. Thus, both modes are associated with latitudinal shifts of the ITCZ, the dipole mode somewhat more strongly than the equatorial one.

To investigate the frequency dependence of the relationships suggested by the correlations, Figure 4 displays the results of a coherence analysis among the three indices (Bloomfield, 1976). Coherence (COH) is high (i.e., above the 80% confidence limit, COH > 0.61, calculated according to Chapter 5 of Emery and Thomson, 1998) between ΔSST and ΔZ20 in the decadal band and at periods from 1–2 years. It is low at intermediate periods (3–4 years), which are typical periods for the "Atlantic El Niño" (Zebiak, 1993). Coherence is high between ΔSST and ΔITCZ throughout much of the frequency domain, especially in the decadal period where the coherence increases to the 90% level (COH > 0.78). Thus, the SST dipole is correlated with the latitudinal shifts in the trade-wind system at almost all frequencies. In contrast, the coherence between ΔZ20 and ΔITCZ is similar in structure to that between ΔZ20 and ΔSST, being high at decadal and 1–2 year bands and low at intermediate periods.

The correlation of SST north and south of the equator was calculated. We obtained a correlation coefficient of 0.18 between the SST averaged north of 5N and the Z20 (SST leading by 1 month), and -0.48 between the SST averaged south of 5N and the Z20 (SST leading by 1 month). In our definition of a dipole (c.f. Servain, 1991), the southern hemisphere SST index used includes the equatorial band, which would explain why it is better correlated with the equatorial mode. Further work is in progress to clarify, using yet stronger observational evidence the ambiguities around the relationship between the various indices.

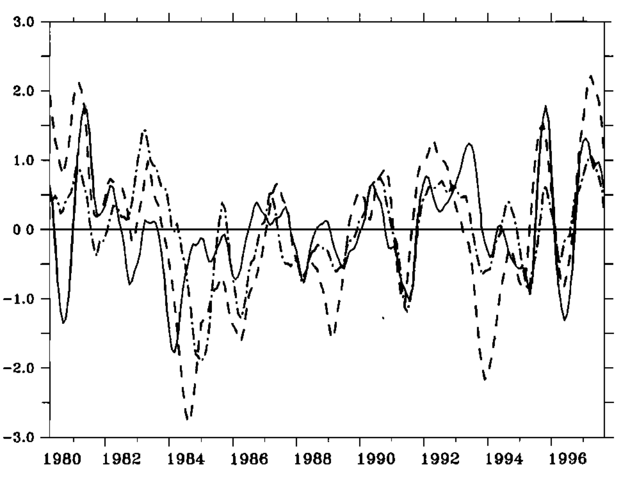

Figure 3. Monthly time series of ΔZ20 (solid line), ΔSST (dashed line), and ΔITCZ (dashed/dotted line) from the observations for the period 1980–1997. ΔZ20 is an index of the changes in the equatorial thermocline west-east slope, ΔSST measures the north-south SST gradient, ΔITCZ identifies the changes in the latitudinal position of ITCZ. Each time series is smoothed by a 6-month running-mean filter.

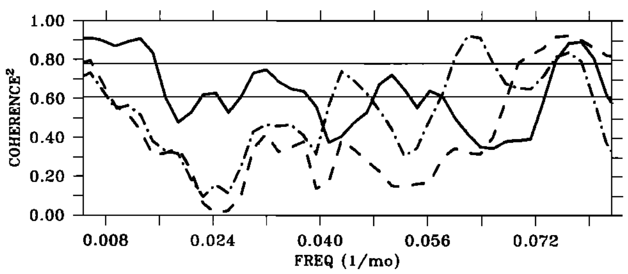

Figure 4. Coherence plots for ΔITCZ vs. ΔSST (solid curve), ΔITCZ vs. ΔZ20 (dashed line) and ΔSST vs. ΔZ20 (dashed-dotted line) as a function of frequency. The two straight lines represent the 80% and 90% significance levels.

Concluding Remarks

It is shown that the equatorial and dipole modes, the two main modes of climatic variability in the tropical Atlantic, as well as the latitudinal position of the ITCZ, are linked at decadal and short-interannual (1–2 years) time scales. These linkages indicate that the processes involved are much the same as those that control the seasonal cycle. They suggest, for example, the following scenario for the positive phase of an oscillation: An anomalous northward displacement of the ITCZ (ΔITCZ > 0) is associated with a similar displacement of the entire trade-wind system. This shift weakens the northeast trades, and strengthens the southeast trades both south of and along the equator. These changes in turn increase the equatorial thermocline tilt (ΔZ20 > 0), warm SST north of the ITCZ due to a decrease in evaporative cooling, and cool it in the southern and equatorial regions due to latent-heat loss, somewhat more strongly in the eastern equatorial ocean due to increased upwelling there (ΔSST > 0). This anomalous condition favors droughts in the Nordeste region and along the continental border of the Gulf of Guinea, and enhances rainfall in the Sahel.

It is interesting that at intermediate (2–4 years) scales there is little coherence between the equatorial mode and either the SST dipole or ITCZ variation. This property suggests that in this band the equatorial mode is generated by a mechanism different from the one outlined in the previous paragraph. Possibilities include another internal mechanism such as the one proposed by Zebiak (1993), or external forcing such as occurs during ENSO. Further analyses, including multi-annual numerical simulations, are needed to sort out the dynamics suggested by these linkages. We are currently working to obtain a better understanding of the dynamic and thermodynamic processes that govern the two modes at all frequencies.

Acknowledgements. The XBT data were collected, validated and archived at the TOGA-WOCE Centre in Brest, France. The numerical simulation was performed by Christophe Maés at the "Laboratoire d'Océanologie Dynamique et de Climatologie" (LODYC/UMR 121) of l'Université de Paris 6, France, and results were made available to us by Claire Levy. We would like to thank Pascale Delécluse and Jon Ahlquist for helpful discussions during this research, and two anonymous reviewers for their comments and suggestions, which were useful in improving the discussion of our results. This work was supported in part by COFECUB agreement No. 27/96-99, by CNPq grant 300223/93-5 RN, and by NOAA grant NA76GP0353 through the GOALS program.

References

Bloomfield, P., Fourier analysis of time series: An introduction, Chapter 9, *John Wiley & Sons.*, 258pp., 1976.

Carton, J. A., Cao, X., Giese, B. S., and da Silva, A. M., Decadal and interannual SST variability in the tropical Atlantic, *J. Phys. Oceanogr.*, 26, 1165-1175, 1996.

Chang, P., Ji, L., and Li, H., A decadal climate variation in the tropical Atlantic Ocean from thermodynamic air-sea interactions, *Nature*, 385, 516-518, 1997.

Delécluse, P., Madec, G., Imbard, M., and Levy, C., OPA version 7 ocean general circulation model reference manual, *Rapport Interne LODYC 93/05*, 111pp., [Available from LODYC, Université Paris VI, 75252 Paris, France], 1993.

Emery, W. J., and Thomson, R. E., Data analysis method in physical oceanography (Chapter 5: Time-series analysis methods), *Pergamon Press.*, (ISBN: 0080314341), 634pp., 1998.

Fabri, M. C., Dessier, A., Maudire, G., Raguenes, Y., and Rebert, J.-P., Global subsurface data Centre (GSDC) for TOGA and WOCE, *International WOCE Newsletter*, 22, 18-20, 1996.

Folland, C., Palmer, T., and Parker, D., Sahel rainfall and world-wide sea temperature 1901-85, *Nature*, 320, 602-606, 1986.

Hisard, P., Observation de réponses de type "El-Niño" dans l'Atlantique tropical, Golfe de Guinée, *Oceanologica Acta*, 3, 69-78, 1980.

Houghton, R. W., and Tourre, Y., Characteristics of low-frequency sea surface temperature fluctuations in the tropical Atlantic, *J. Climate*, 5, 765-771, 1992.

Katz, E. J., Equatorial Kelvin waves in the Atlantic, *J. Geophys. Res.*, 92, 1894-1898, 1987.

Katz, E. J., Waves along the equator in the Atlantic, *J. Phys. Oceanogr.*, 27, 2536-2544, 1997.

McCreary, J. P., Picaut, J., and Moore, D. W., Effects of remote annual forcing in the eastern tropical Atlantic Ocean, *J. Mar. Res.*, 42, 45-81, 1984.

Mehta, V. M., and Delworth, T., Decadal variability of the tropical Atlantic Ocean surface temperature in shipboard measurements and in a global ocean-atmosphere model, *J. Climate*, 8, 172-190, 1995.

Moore, D. W., Hisard, P., McCreary, J., Merle, J., O'Brien, J., Picaut, J., Verstraete, J. M., and Wunsch, C., Equatorial adjustment in the eastern Atlantic, *Geophys. Res. Lett.*, 5, 637-640, 1978.

Moura, A. D., and Shukla, J., On the dynamics of droughts in northeast Brazil: observations, theory and numerical experiments with a general circulation model, *J. Atmos. Sci.*, 38, 2653-2675, 1981.

Nobre, P., and Shukla, J., Variations of sea surface temperature, wind stress, and rainfall over the tropical Atlantic and South America, *J. Climate*, 9, 2464-2579, 1996.

Philander, S. G. H., Variability of the tropical oceans, *Dyn. Atmos. Ocean*, 3, 191-208, 1979.

Picaut, J., Propagation of the seasonal upwelling in the eastern equatorial Atlantic, *J. Phys. Oceanogr.*, 13, 18-37, 1983.

Rajagopalan, B., Kushnir, Y., and Tourre, Y., Observed decadal midlatitude and tropical Atlantic variability, *Geophys. Res. Lett.*, 25, 3967-3970, 1998.

Reverdin, G., Delécluse, P., Lévy, C., Andrich, P., Morlière, A., and Verstraete, J. M., The near surface tropical Atlantic in 1982-1984. Results from a numerical simulation and a data analysis, *Prog. Oceanogr.*, 27, 273-340, 1991.

Servain, J., Simple climatic indices for the tropical Atlantic Ocean and some applications, *J. Geophys Res.*, 96, 15.137-15.146, 1991.

Servain, J., and Arnault, S., On forecasting abnormal climatic events in the tropical Atlantic Ocean, *Ann. Geophysicae*, 13, 995-1008, 1995.

Servain, J., and Merle, J., Interannual climate variations over the tropical Atlantic Ocean, *NATO ASI Series*, Vol. 16, Prediction of Interannual Climate Variations, Edited by J. Shukla, © Springer-Verlag Berlin Heidelberg, 153-171, 1993.

Servain, J., Picaut, J., and Busalacchi, A.J., Interannual and seasonal variability of the tropical Atlantic Ocean depicted by sixteen years of sea surface temperature and wind stress, J.C.J. Nihoul (Editor), *Coupled Ocean-Atmosphere Models*, © Elsevier Science Publishers B.V, Amsterdam, Netherlands, 211-237, 1985.

Servain, J., Stricherz, J. N., and Legler, D. M., TOGA Pseudo-stress Atlas 1985-1994 - Vol 1: Tropical Atlantic, *Edited by Centre ORSTOM de Brest, France,* 162pp., 1996.

Wainer, I., and Soares, J., North Northeast Brazil rainfall and its decadal – scale relationship to wind stress and sea surface temperature, *Geophys Res. Letters.*, 24, 277-280, 1997.

Zebiak, S. E., Air-sea interaction in the equatorial Atlantic region, *J. Climate*, 6, 1567-1586, 1993.

J. Servain and A. Dessier, Centre ORSTOM, B.P. 70, 29280, Plouzané, France. (e-mail: servain@orstom.fr; dessier@orstom.fr)

I. Wainer, Dept. Oceanográfia Fisíca, Universidade de São Paulo, Praça do Oceanográfico 191 05508-900, São Paulo, Brasil. (e-mail: wainer@usp.br)

J. P. McCreary, Oceanographic Center, Nova Southeastern University, 8000 N. Ocean Dr., Dania, FL 33004, USA. (e-mail: jay@nsu.acast.nova.edu)

(Received May 28, 1998; revised December 11, 1998; accepted December 31, 1998.)